PHYSICAL REVIEW D **76,** 075016 (2007)

# Four generations and Higgs physics

Graham D. Kribs,[1] Tilman Plehn,[2] Michael Spannowsky,[3] and Tim M. P. Tait[4]

[1]*Department of Physics and Institute of Theoretical Science, University of Oregon, Eugene, Oregon 97403, USA*
[2]*SUPA, School of Physics, University of Edinburgh, Edinburgh EH9 3JZ, Scotland*
[3]*ASC, Department für Physik, Ludwig-Maximilians-Universität München, 80333 München, Germany*
[4]*HEP Division, Argonne National Laboratory, 9700 Cass Avenue, Argonne, Illinois 60439, USA*

(Received 24 July 2007; published 26 October 2007)

In the light of the LHC, we revisit the implications of a fourth generation of chiral matter. We identify a specific ensemble of particle masses and mixings that are in agreement with all current experimental bounds as well as minimize the contributions to electroweak precision observables. Higgs masses between 115–315 (115–750) GeV are allowed by electroweak precision data at the 68% and 95% C.L. Within this parameter space, there are dramatic effects on Higgs phenomenology: production rates are enhanced, weak-boson-fusion channels are suppressed, angular distributions are modified, and Higgs pairs can be observed. We also identify exotic signals, such as Higgs decay to same-sign dileptons. Finally, we estimate the upper bound on the cutoff scale from vacuum stability and triviality.

DOI: 10.1103/PhysRevD.76.075016 PACS numbers: 12.60.−i, 14.80.Bn

## I. INTRODUCTION

New physics that affects the observability of the Higgs boson of the standard model (SM) is of utmost importance to study. One of the simplest kinds of new physics is a sequential replication of the three generations of chiral matter [1]. Such a fourth generation has been considered and forgotten or discarded many times, wrongly leaving the impression that it is either ruled out or highly disfavored by experimental data (for instance, see Ref. [2]).

The status of four generations is more subtle [3]. Reference [4] analyzed the contributions of one (and more) extra generations to the oblique parameters and explicitly found that one generation can be perfectly consistent with a heavy (500 GeV) Higgs. These significant results are primarily based on numerical scans, with emphasis on the role of a lighter neutrino (50 GeV) to minimize the contributions to the oblique parameters (see also Ref. [5]). However, a neutrino with mass of 50 GeV, if unstable, is ruled out by LEP II bounds, while if it is exactly stable, may be ruled out by dark matter direct search experiments [6]. Correlations of the mass parameters leading to viable spectra are certainly not transparent, making it hard to determine how to parse their results against present experimental bounds.

Subsequent analyses [7,8] studied the relationships among fourth-generation parameters, but their analysis was performed using a global (numerical) fit to 2001 electroweak data and again emphasized a 50 GeV neutrino. Electroweak data has since been refined (in particularly $M_W$), so these results no longer obviously apply, in particular, if we incorporate a heavier neutrino. The impact of a chiral fourth generation on Higgs physics has been briefly discussed [9–12], however the range of masses that were considered were not necessarily correlated to the fourth-generation mass spectra and Higgs mass appropriate to satisfy current direct search bounds and electroweak precision constraints. Moreover, in cases where there is overlap, our results do not always agree; we point out the differences below.

In this paper, we first systematically determine the allowed parameter space of fourth-generation masses and mixings. We find quite simple mass relations that minimize the precision electroweak oblique parameters, so our analysis can easily be extended to future refinements in electroweak measurements. We then use typical spectra to compute the consequences for fourth-generation particle production and decay, as well as the effects on the Higgs sector of the standard model. We find that a wide range of Higgs masses is consistent with electroweak data, leading to significant modifications of Higgs production and decay. We outline the major effects, identifying the well-known effects from others that (to our knowledge) are new.

There are in addition spectacular signals of the fourth generation itself. Given that direct searches at LEP II and Tevatron have already constrained the masses somewhat, we can expect future searches at Tevatron will continue to push the limits up, but will not rule out four generations. The LHC is able to probe heavy quarks throughout their mass range. Many of the signals have been recently considered (albeit in somewhat different mass ranges and context from what we consider here) in Refs. [13,14], to which we refer the interested reader.

## II. FOUR GENERATIONS

The framework we consider is to enlarge the standard model to include a complete sequential fourth generation of chiral matter ($Q_4$, $u_4$, $d_4$, $L_4$, $e_4$) as well as a single right-handed neutrino $\nu_4$. Yukawa couplings and right-handed neutrino masses are given by

$$\mathcal{L} = y^u_{pq}\bar{Q}_p H u_q + y^d_{pq}\bar{Q}_p H^\dagger d_q + y^e_{pq}\bar{L}_p H^\dagger e_q + y^\nu_{pq}\bar{L}_p H \nu_q + \frac{1}{2}M_{pq}\bar{\nu}^c_p \nu_q + \text{H.c.} \quad (1)$$

 

The generation indices are $p, q = 1, 2, 3, 4$ while we reserve $i, j = 1, 2, 3$ for the standard model. SU(2) contractions are implicit. Light neutrino masses can arise from either a hierarchy in neutrino Yukawa couplings $y^\nu_{ij} \ll y_{44}$ or right-handed neutrino masses $M_{ij} \gg M_{44}$ or some combination. (For an amusing combination, see Ref. [15]). We mainly consider two possibilities for the fourth-generation neutrino mass: purely Dirac ($M_{44} = 0$) and mixed ($M_{44} \sim y^\nu_{44} v$).

There are four obvious restrictions on a fourth generation: (1) the invisible width of the $Z$; (2) direct search bounds; (3) generational mixing; (4) oblique electroweak effects. We now discuss them one by one.

Once a fourth-generation neutrino has a mass $m_\nu \gtrsim M_Z/2$, the constraint from the invisible $Z$ width becomes moot. Assuming nonzero mixings $y_{i4}$ or $M_{i4}$, the fourth-generation quarks, charged lepton, and neutrino decay, and thus there are no cosmological constraints from stable matter. (We will briefly comment on neutrino dark matter at the end this paper.)

A robust lower bound on fourth-generation masses comes from LEP II. The bound on unstable charged leptons is 101 GeV, while the bound on unstable neutral Dirac neutrinos is (101, 102, 90) GeV for the decay modes $\nu_4 \to (e, \mu, \tau) + W$. These limits are weakened only by about 10 GeV when the neutrino has a Majorana mass. Because the small differences in the bounds between different flavors, charged versus neutral leptons, and Majorana versus Dirac mass do not affect our results, we apply the LEP II bounds (which also include similar bounds on quarks, for example [2,16]) as $m_{\nu_4, \ell_4, u_4, d_4} \gtrsim 100$ GeV throughout.

The Tevatron has significantly greater sensitivity for fourth-generation quarks [17]. The strongest bound is from the CDF search for $u_4 \bar{u}_4 \to q\bar{q}W^+W^-$, obtaining the lower bound $m_{u_4} > 258$ GeV to 95% confidence level (C.L.) [18]. No $b$ tag was used, so there is no dependence on the final-state jet flavor, and hence this limit applies independent of the Cabibbo-Kobayashi-Maskawa (CKM) elements $V_{u_4 i}$. There is no analogous limit on the mass of $d_4$ beyond the LEP II bound [19]. If $m_{d_4} > m_t + m_W$ and $|V_{td_4}| \gg |V_{ud_4}|, |V_{cd_4}|$, then the dramatic $d_4 \bar{d}_4 \to t\bar{t}WW$ signal may be confused into the top sample. If the decay proceeds through a lighter generation, then the production rate and signal are the same as for $u_4$, and so we expect a bound on the mass of $d_4$ similar to that on $u_4$. If $m_{d_4} < m_t + m_W$, then $d_4$ decay could proceed through a "doubly-Cabbibo" suppressed tree-level process $d_4 \to cW$ or through the one-loop process $d_4 \to bZ$. The relative branching ratios (BRs) depend on details [20,21]. In particular, taking $\mathrm{BR}(d_4 \to bZ) = 1$, CDF obtains the bound $m_{d_4} > 268$ GeV at 95% C.L. [22]. We choose to adopt the largely CKM-independent bound $m_{u_4, d_4} > 258$ GeV throughout.

The off-diagonal elements $V_{u_4 i}, V_{j d_4}$ of the CKM matrix $V = y^{u\dagger} y^d$ are constrained by flavor physics. As in the standard model, the flavor-violating neutral current effects occur in loops and are automatically Glashow-Iliopoulos-Maini (GIM) suppressed. Rough constraints on the mixing between the first/second and fourth generation can be extracted requiring unitarity of the enlarged $4 \times 4$ CKM matrix. The SM $3 \times 3$ submatrix is well tested by a variety of SM processes [2]. The first row of the matrix, combined with measurements of $V_{ud}$, $V_{us}$, and $V_{ub}$, yields

$$|V_{ud_4}|^2 = 1 - |V_{ud}|^2 - |V_{us}|^2 - |V_{ub}|^2 \simeq 0.0008 \pm 0.0011. \quad (2)$$

For the second row we can use the hadronic $W$ branching ratio and other data to obtain

$$|V_{cd_4}|^2 = 1 - |V_{cd}|^2 - |V_{cs}|^2 - |V_{cb}|^2 \simeq -0.003 \pm 0.027. \quad (3)$$

Similarly, the first column of the matrix allows one to infer

$$|V_{u_4 d}|^2 = 1 - |V_{ud}|^2 - |V_{cd}|^2 - |V_{td}|^2 \simeq -0.001 \pm 0.005. \quad (4)$$

More stringent constraints can be obtained with specific processes. For exmaple, Ref. [23] found that the recent observation of $D^0$-$\bar{D}^0$ mixing leads to the constraint $|V_{ud_4} V_{cd_4}| \lesssim 0.002$. If we require all of these constraints on the additional CKM elements be satisfied to $1\sigma$, we find

$$|V_{ud_4}|, |V_{u_4 d}|, |V_{cd_4}| \lesssim 0.04. \quad (5)$$

This size is, nevertheless, still significantly larger than the smallest elements in the CKM matrix $|V_{ub}|, |V_{td}|$. The remainder of the elements ($V_{td_4}$, $V_{u_4 s}$, $V_{u_4 b}$, and $V_{u_4 d_4}$) could be constrained through a global fit to the $4 \times 4$ CKM matrix, including the contributions of the fourth-generation quarks to specific observables in loops (for example [24,25]), but this is beyond the scope of this work. Similarly there are two additional $CP$-violating phases in the $4 \times 4$ CKM matrix, but since their effects are proportional to the unknown (real parts) of the off-diagonal CKM mixings, we ignore their effects.

The least constrained sector is the mixing between the third and fourth generations. The observation of single top production [26,27] can be used to obtain a lower limit $|V_{tb}| > 0.68$ at 95% C.L. [26], which still allows for comparatively large third/fourth generation mixing. Combining the restrictions on a fourth generation from electroweak precision data (next section) with the $4 \times 4$ CKM unitarity constraints may yield an even stronger bound, $|V_{tb}| \gtrsim 0.8$ [28]. Thus it seems likely that fourth generation charged-current decays will be mostly into third generation quarks, provided the mass difference is large enough to permit two-body decays.

The new elements in the Pontecorvo-Maki-Nakagawa-Sakata (PMNS) matrix $U = y^{\nu\dagger} y^e$ also have constraints from lepton flavor violation in the charged and neutral

sectors. One rather stringent constraint comes from the nonobservation of $\mu \to e\gamma$. For weak-scale purely Dirac neutrinos this constraint is straightforward to estimate using [29]; we obtain $|U_{e4}U_{\mu 4}| \lesssim 4 \times 10^{-4}$. An even stronger constraint can be obtained from $\mu \to e$ conversion in nuclei; Ref. [30] obtains $|U_{e4}U_{\mu 4}| \lesssim 5 \times 10^{-5}$ for weak-scale right-handed neutrinos, and we expect that this bound also (approximately) applies to weak-scale Dirac neutrinos. This suggests that first/second generation mixings with the fourth generation need to be a bit smaller than about 0.01 to satisfy all constraints. Other generational mixings can also be constrained from the absence of lepton flavor-violating effects, where again third/fourth generation mixings are (as expected) the most weakly constrained.

There is, however, a significant constraint from neutrinoless double beta decay on $|U_{i4}|$ in the presence of a weak-scale Majorana mass $M_{44}$. Such a decay can be mediated by a very light neutrino mixing with a weak-scale (partly) Majorana neutrino. Using Ref. [31] and assuming only first/fourth generational mixing, we obtain

$$\frac{|U_{e4}|^2 p_F^2 M_{44}}{3m_D^2} \lesssim \text{eV}, \tag{6}$$

where $m_D = y^\nu_{44} v$ and PMNS phases are ignored. This expression is valid as long as the fourth-generation neutrino masses exceed the characteristic energy scale of the double-beta nuclear process, $m_{\nu_{1,2}} \gg p_F \simeq 60$ MeV. Inserting characteristic values, we obtain

$$|U_{e4}| \lesssim 0.9 \times 10^{-2} \frac{m_D}{M_{44}^{1/2}(100\ \text{GeV})^{1/2}}. \tag{7}$$

No bound remains once the fourth-generation Majorana mass is made small, $M_{44} \lesssim 10$ MeV.

## III. ELECTROWEAK CONSTRAINTS

The most pernicious effect of a fourth generation is the contribution to oblique electroweak corrections. $B \leftrightarrow W^3$ mixing is enhanced, leading to a positive contribution $\Delta S = 0.21$ in the limit of degenerate isospin multiplets (quark and lepton). Degeneracy is usually assumed for simplicity since split doublets significantly contribute to the isospin violating parameter $T$.

There are three important effects that can mitigate the contribution to $\Delta S$. The first, and most important, is exploiting the relative experimental insensitivity to the $\Delta S \simeq \Delta T$ direction in oblique parameter space. We will be more precise below, but suffice to say slightly split electroweak doublets are in far better agreement with electroweak data than without the $\Delta T$ contribution. The second effect involves a reduced contribution to $S$ by splitting the fourth-generation multiplets in a particular mass hierarchy. The last, and least important effect is introducing a Majorana mass for the fourth-generation neutrino.

Splitting the up-type from down-type fermion masses in the same electroweak doublet can give a negative contribution to $S$. In the large mass limit $m_{u,d} \gg M_Z$, the contribution to $S$ depends logarithmically on the ratio $m_u/m_d$ [4,32]

$$\Delta S = \frac{N_c}{6\pi}\left(1 - 2Y \ln\frac{m_u^2}{m_d^2}\right), \tag{8}$$

where $Y$ is the hypercharge of the left-handed doublet of fermions with degeneracy (color factor) $N_c$. Clearly the fourth-generation contributions to $S$ are reduced if $m_{u_4}/m_{d_4} > 1$ for quarks ($Y = 1/6$) and $m_\nu/m_\ell < 1$ for leptons ($Y = -1/2$). How big can this effect be given that split multiplets also contribute to $\Delta T$?

To calculate $\Delta S$ (and $\Delta T$ and $\Delta U$) we use exact one-loop expressions which are valid for all $m_{u,d}$ [33]. We checked our formulas by explicitly verifying finiteness (renormalization scale independence) as well as finding numerical agreement with several explicit results given in Ref. [4]. In Fig. 1 we show the size of the contribution from the $(u_4, d_4)$ doublet as a function of the masses of the quarks. The effect of using the exact one-loop expressions is modest; in fact Eq. (8) reproduces the $S$ contours up to an accuracy $\pm 0.01$ throughout the plot. The typical size of $U$ is smaller than 0.02 everywhere, and so we set $U = 0$ throughout.

For the leptons, what is most important is the split between the neutral and charged fermion masses. For example, $m_{\nu,\ell} \simeq 100, 135$ GeV implies $(\Delta S_\nu, \Delta T_\nu) \simeq (0.02, 0.02)$, and the slightly larger values $m_{\nu,\ell} \simeq 100, 155$ GeV give $(\Delta S_\nu, \Delta T_\nu) \simeq (0.00, 0.05)$. These re-

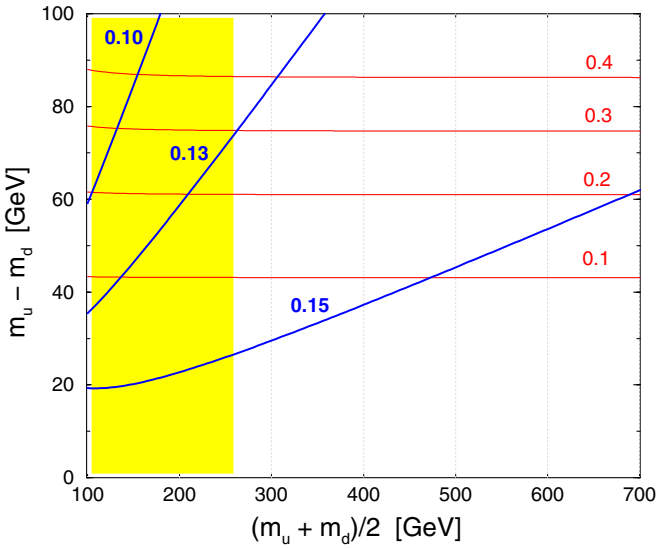


FIG. 1 (color online). Contours of constant $\Delta S_q$ (diagonal blue lines) and $\Delta T_q$ (horizontal red lines) for the fourth-generation quarks. The plot is symmetric with respect to $m_{u_4} - m_{d_4} \leftrightarrow m_{d_4} - m_{u_4}$, since $\Delta T_q$ is positive definite. The Tevatron bound $m_{u_4,d_4} > 258$ GeV excludes the shaded (yellow) region.

sults from the exact one-loop formulas agree surprisingly well with Eq. (8), despite the lepton masses being near $M_Z$.

Fits of the combined electroweak data provide constraints on the oblique parameters and have been performed by the LEP Electroweak Working Group (LEP EWWG) [34] and separately by the PDG [2]. Both fits find that the standard model defined by $(S, T) = (0, 0)$ with $m_t = 170.9$ GeV and $m_H = 115$ GeV is within $1\sigma$ of the central value (always holding $U = 0$). However, the two fits disagree on the best-fit point. The latest LEP EWWG fit finds a central value $(S, T) = (0.06, 0.11)$ [35] with a 68% contour that is elongated along the $S \simeq T$ major axis from $(S, T) = (-0.09, -0.03)$ to $(0.21, 0.25)$. By contrast, the PDG find the central value $(S, T) = (-0.07, -0.02)$ after adjusting $T$ up by $+0.01$ to account for the latest value of $m_t = 170.9$ GeV.

The most precise constraints on $S$ and $T$ arise from $\sin^2\theta^{\text{eff}}_{\text{lept}}$ and $M_W$, used by both groups. The actual numerical constraints derived from these measurements differ slightly between each group, presumably due to slight updates of data (the $S$-$T$ plot generated by the 2006 LEP EWWG is 1 yr newer than the plot included in the 2006 PDG). A larger difference concerns the use of the $Z$ partial widths and $\sigma_h$. The LEP EWWG advocate using just $\Gamma_\ell$, since it is insensitive to $\alpha_s$. This leads to a flatter constraint in the $S$-$T$ plane. The PDG include the $\alpha_s$-sensitive quantities $\Gamma_Z$, $\sigma_h$, $R_q$ as well as $R_\ell$, and obtain a less flat, more oval-shaped constraint. Additional lower-energy data can also be used to (much more weakly) constrain $S$ and $T$, although there are systematic uncertainties (and some persistent discrepancies in the measurements themselves). The LEP EWWG do not include lower-energy data in their fit, whereas the PDG appear to include some of it. In light of these subtleties, we choose to use the LEP EWWG results when quoting levels of confidence of our calculated shifts in the $S$-$T$ plane. We remind the reader, however, that the actual level of confidence is obviously a sensitive function of the precise nature of the fit to electroweak data.

TABLE I. Examples of the total contributions to $\Delta S$ and $\Delta T$ from a fourth generation. The lepton masses are fixed to $m_{\nu_4} = 100$ GeV and $m_{\ell_4} = 155$ GeV, giving $\Delta S_{\nu\ell} = 0.00$ and $\Delta T_{\nu\ell} = 0.05$. The best fit to data is $(S, T) = (0.06, 0.11)$ [35]. The standard model is normalized to $(0, 0)$ for $m_t = 170.9$ GeV and $m_H = 115$ GeV. All points are within the 68% C.L. contour defined by the LEP EWWG [35].

| Parameter set | $m_{u_4}$ | $m_{d_4}$ | $m_H$ | $\Delta S_{\text{tot}}$ | $\Delta T_{\text{tot}}$ |
|---|---|---|---|---|---|
| (a) | 310 | 260 | 115 | 0.15 | 0.19 |
| (b) | 320 | 260 | 200 | 0.19 | 0.20 |
| (c) | 330 | 260 | 300 | 0.21 | 0.22 |
| (d) | 400 | 350 | 115 | 0.15 | 0.19 |
| (e) | 400 | 340 | 200 | 0.19 | 0.20 |
| (f) | 400 | 325 | 300 | 0.21 | 0.25 |

In Table I we provide several examples of fourth-generation fermion masses which yield contributions to the oblique parameters that are within the 68% C.L. ellipse of the electroweak precision constraints. We illustrate the effect of increasing Higgs mass with compensating contributions from a fourth generation in Fig. 2. More precisely, the fit to electroweak data is in agreement with the existence of a fourth generation and a light Higgs about as well as the fit to the standard model alone with $m_H = 115$ GeV. Using suitable contributions from the fourth-generation quarks, heavier Higgs masses up to 315 GeV remain in agreement with the 68% C.L. limits derived from electroweak data. Heavier Higgs masses up to 750 GeV are permitted if the agreement with data is relaxed to the 95% C.L. limits.

Until now we have focused on purely Dirac neutrinos. However, there is also a possible reduction of $S_{\text{tot}}$ when the fourth-generation neutrino has a Majorana mass comparable to the Dirac mass [36,37]. Using the exact one-loop expressions of Ref. [37], we calculated the contribution to the electroweak parameters with a Majorana mass. Given the current direct-search bounds from LEP II on unstable neutral and charged leptons, we find a Majorana mass is unfortunately not particularly helpful in significantly lowering $S$. A Majorana mass does, however, enlarge the parameter space where $S \simeq 0$. For example, given the lepton Dirac and Majorana masses $(m_D, M_{44}) = (141, 100)$ GeV, the lepton mass eigenstates are $(m_{\nu_1}, m_{\nu_2}, m_\ell) = (100, 200, 200)$ GeV, and contributions

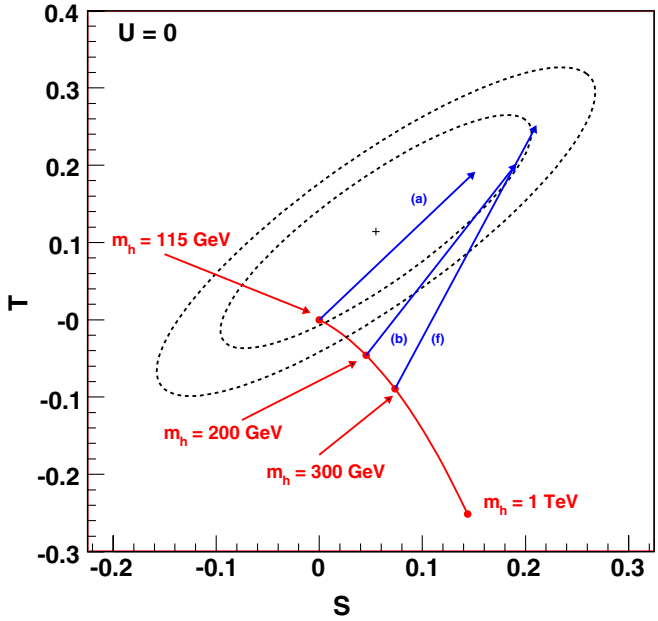


FIG. 2 (color online). The 68% and 95% C.L. constraints on the $(S, T)$ parameters obtained by the LEP Electroweak Working Group [34,35]. The shift in $(S, T)$ resulting from increasing the Higgs mass is shown in red (solid line). The shifts in $\Delta S$ and $\Delta T$ from a fourth generation with several of the parameter sets given in Table I are shown in blue (arrow lines).

to the oblique parameters of $(\Delta S_\nu, \Delta T_\nu) = (0.01, 0.04)$. It is difficult to find parameter regions with $\Delta S_\ell < 0$ without either contributing to $\Delta U_\ell \simeq -\Delta S_\ell$, contributing significantly more to $\Delta T_\ell$, or taking $m_{\nu_1} < 100$ GeV which violates the LEP II bound for unstable neutrinos.

Let us summarize our results thus far. We have identified a region of fourth-generation parameter space in agreement with all experimental constraints and with minimal contributions to the electroweak precision oblique parameters. This parameter space is characterized by

$$\begin{aligned} m_{\ell_4} - m_{\nu_4} &\simeq 30 - 60 \text{ GeV} \\ m_{u_4} - m_{d_4} &\simeq \left(1 + \frac{1}{5}\ln\frac{m_H}{115 \text{ GeV}}\right) \times 50 \text{ GeV} \\ |V_{ud_4}|, |V_{u_4 d}| &\lesssim 0.04 \qquad |U_{e4}|, |U_{\mu 4}| \lesssim 0.01, \end{aligned} \tag{9}$$

and subject to the current direct search limits $m_{\nu_4,\ell_4} > 100$ GeV and $m_{u_4,d_4} > 258$ GeV. The other elements of the CKM and PMNS matrix are not strongly constrained. The smallest contribution to the oblique parameters occurs for small Higgs masses. The leptons and quark masses are not significantly split, in particular, the two-body decays $\ell_4 \to \nu_4 W$ and $d_4 \to u_4 W$ generally do not occur. Finally, while there are strong restrictions on the mass *differences* between the up-type and down-type fields, there are much milder restrictions on the *scale* of the mass.

## IV. HIGGS SEARCHES

The set of mixing elements and mass hierarchies shown in Eq. (9) has significant effects on Higgs searches at the Tevatron and at the LHC. One clear observation is that Higgs decays into fourth-generation particles, if possible at all, are expected only into leptons, unless the Higgs is exceptionally heavy which is disfavored by precision data.

A fourth generation with two additional heavy quarks is well known to increase the effective $ggH$ coupling by roughly a factor of 3, and hence to increase the production cross section $\sigma_{gg\to H}$ by a factor of roughly 9 [38]. The Yukawa coupling exactly compensates for the large decoupling quark masses in the denominator of the loop integral [39]. This result is nearly independent of the mass of the heavy quarks, once they are heavier than the top. (Modifications to the Higgs production cross section has also been considered in an effective theory approach in Ref. [40].) This enhancement allowed CDF and D0 to very recently rule out a Higgs in a four-generation model within the mass window of roughly $145 < m_H < 185$ GeV to 95% C.L. using the process $gg \to h \to W^+W^-$ [41,42]. While over recent years weak-boson production has proven the leading discovery channels for light Higgs bosons—in the standard model as well as in extensions with more than one Higgs doublet, like, for example, the MSSM [43]—these channels are less promising in models with a fourth generation, because the loop effects on the $WWH$ couplings are small enough to be ignored in the standard model.

The increase in the $ggH$ coupling dramatically increases the decay rate of $H \to gg$. For Higgs masses lighter than about 140 GeV and no new two-body decays, this decay dominates, but is probably impossible to extract from the two-jet background at the LHC. The presence of this decay effectively suppresses all other two-body decays, including the light-Higgs discovery mode $H \to \tau\tau$, by roughly a factor 0.6. Only once the tree-level decay mode $H \to WW^*$ opens does this suppression vanish. More subtle effects occur for the loop-induced decay $H \to \gamma\gamma$. The partial widths for $H \to \gamma\gamma$ and $H \to gg$ can be written as [39]

$$\begin{aligned} \Gamma_{H\to\gamma\gamma} &= \frac{G_\mu \alpha^2 m_H^3}{128\sqrt{2}\pi^3} \left| \sum_f N_c Q_f^2 A_f(\tau_f) + A_W(\tau_W) \right|^2 \\ \Gamma_{H\to gg} &= \frac{G_\mu \alpha_s^2 m_H^3}{36\sqrt{2}\pi^3} \left| \frac{3}{4} \sum_f A_f(\tau_f) \right|^2, \end{aligned} \tag{10}$$

where $A_f$ and $A_W$ are the form factors for the spin-$\frac{1}{2}$ and spin-1 particles, respectively. These form factors are

$$\begin{aligned} A_f(\tau) &= 2[\tau + (\tau - 1) f(\tau)]\tau^{-2} \\ A_W(\tau) &= -[2\tau^2 + 3\tau + 3(2\tau - 1) f(\tau)]\tau^{-2} \end{aligned} \tag{11}$$

with $\tau_i = m_H^2/4m_i^2$ $(i = f, W)$ and $f(\tau)$ defined as the three-point integral

$$f(\tau) = \begin{cases} \arcsin^2\sqrt{\tau} & \tau \le 1 \\ -\frac{1}{4}[\ln\frac{1+\sqrt{1-\tau^{-1}}}{1-\sqrt{1-\tau^{-1}}} - i\pi]^2 & \tau > 1. \end{cases} \tag{12}$$

From the numbers given in Table II we see that the $ggH$ coupling indeed consists of nearly identical contributions from the SM top quark and the two additional fourth-generation quarks. In particular, the contributions of the fourth-generation quarks in the parameters points (a) and (b) are well described by the decoupling limit in which we estimated the enhancement of the Higgs production rate as a factor of 9. For a 200 GeV Higgs we start to observe very small top-mass effects. This means that the enhancement factor in $\sigma_{gg}$ slowly decreases from 8.5 to 7.7 for Higgs masses between 200 and 300 GeV. Of course, this scaling

TABLE II. The dominant form factors for the decay $H \to \gamma\gamma$ and $H \to gg$ according to Eq. (10) for the parameter points (a) and (b). For $H \to gg$ just the quark loops contribute. The form factors are obtained from a modified version of HDECAY [44].

| $m_H$ | 115 | 200 |
|---|---|---|
| $A_W$ | $-8.0321$ | $-9.187 - 5.646i$ |
| $A_t$ | 1.370 | 1.458 |
| $A_{u_4}$ | 1.344 | 1.367 |
| $A_{d_4}$ | 1.349 | 1.382 |
| $A_{\ell_4}$ | 1.379 | 1.491 |

factor breaks down for the top threshold region around 350 GeV and subsequent heavy-quark thresholds. This corresponds to the absorptive imaginary parts of the $A_i$ listed in Table II.

In the standard model the Higgs decay to photons is dominated by the $W$ loop, which destructively interferes with the smaller top loop. In Table II we see how in the fourth-generation model all additional heavy particles contribute to the loop. For a light Higgs boson this implies a suppression of the branching ratio $\mathrm{BR}(\gamma\gamma)$ by roughly a factor 1/9 [45]. Suppression of the $h \to \gamma\gamma$ mode has also been recently considered in a somewhat different context in Ref. [46].

We show the complete set of branching ratios in Fig. 3. All predictions for Higgs decays are computed with a modified version of HDECAY [44] which includes radiative corrections also to the fourth-generation decays, but no off shell effects for these decays. The two thresholds in $\mathrm{BR}(\ell_4\bar{\ell}_4)$ and $\mathrm{BR}(\nu_4\bar{\nu}_4)$ compete with the larger top decay channel with its color factor $N_c$, but all of them are small compared to the gauge boson decays. Higgs decays to fourth-generation quarks are implemented in the extended version of HDECAY but only occur for larger Higgs masses.

For a light Higgs below 200 GeV the effects on different gluon-fusion channels are roughly summarized by

$$\begin{aligned}\sigma_{gg}\,\mathrm{BR}(\gamma\gamma)|_{\mathrm{G4}} &\simeq \sigma_{gg}\,\mathrm{BR}(\gamma\gamma)|_{\mathrm{SM}}\\ \sigma_{gg}\,\mathrm{BR}(ZZ)|_{\mathrm{G4}} &\simeq (5\cdots 8)\sigma_{gg}\,\mathrm{BR}(ZZ)|_{\mathrm{SM}}\\ \sigma_{gg}\,\mathrm{BR}(f\bar{f})|_{\mathrm{G4}} &\simeq 5\sigma_{gg}\,\mathrm{BR}(f\bar{f})|_{\mathrm{SM}}.\end{aligned} \tag{13}$$

In Fig. 4 we show a set of naively scaled discovery contours for a generic compact LHC detector, modifying all known discovery channels according to fourth-generation effects [47]. The enhancement of the production

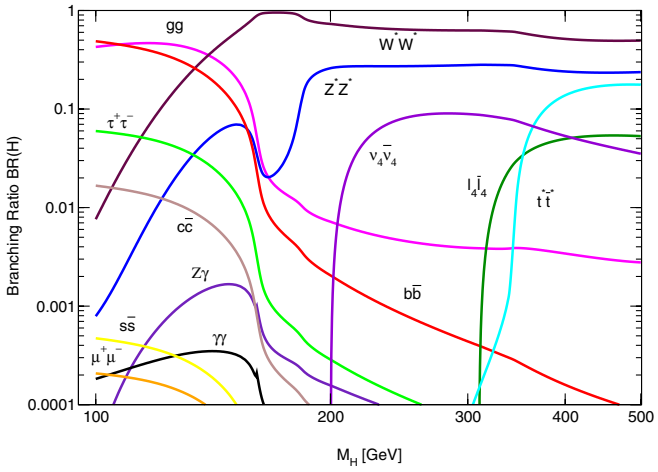


FIG. 3 (color online). Branching ratio of the Higgs with fourth-generation effects assuming $m_\nu = 100$ GeV and $m_\ell = 155$ GeV. The loop effects to $H \to gg$ and $H \to \gamma\gamma$ are largely insensitive to the fourth-generation quark masses. For the fourth-generation masses we follow the reference point (b).

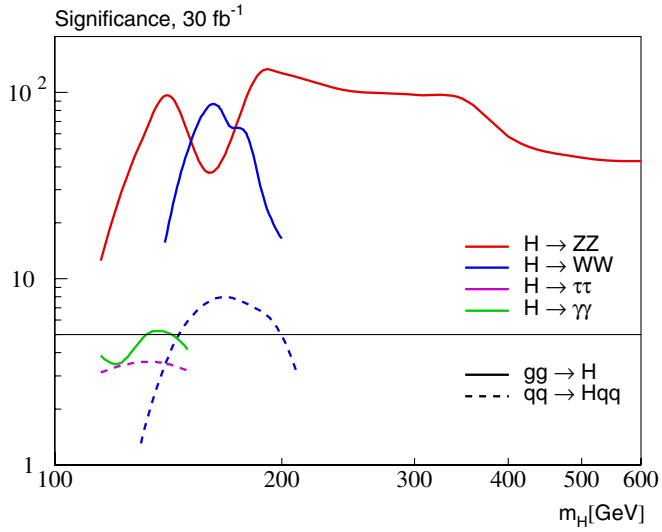


FIG. 4 (color online). Scaled LHC discovery contours for the fourth-generation model. All channels studied by CMS are included. The significances have naively been scaled to the modified production rates and branching ratios using the fourth-generation parameters of reference point (b).

cross section implies the "golden mode" $H \to ZZ \to 4\mu$ can be used throughout the Higgs mass range, from the LEP II bound to beyond 500 GeV. Both $WW$ channels [48,49] are still relevant, but again the gluon-fusion channel (which in CMS analyses for a SM Higgs tends to be more promising that the weak-boson channel, while Atlas simulation shows the opposite [50]) wins due to the fourth-generation enhancement. As mentioned above, the weak-boson-fusion discovery decay $H \to \tau\bar{\tau}$ becomes relatively less important, even though its significance is only slightly suppressed. Weak-boson-fusion production with a subsequent decay to photons is suppressed by one order of magnitude compared to the standard model and not shown anymore, while for the gluon-fusion channel with a decay to photons the corrections to the production rate and the decay width accidentally cancel.

Measuring the relative sizes of the different production and decay modes would allow an interesting study of Higgs properties that should be easily distinguishable from other scenarios (two Higgs doublet model, supersymmetry, etc.). Moreover, there may be novel search strategies for the Tevatron that would be otherwise impossible given just the SM Higgs production rate.

Weak-boson-fusion Higgs production has interesting features beyond its total rate. Most importantly, it has the advantage of allowing us to extract a Higgs sample only based on cuts on the two forward tagging jets, allowing us to observe Higgs decays to taus and even invisible Higgs decays [43,51]. Among the relevant distribution for this strategy are the angular correlations between the tagging jets: for two $W$ bosons coupling to the Higgs proportional to the metric tensor we find that the azimuthal angle

correlation between the tagging jets is flat, modulo slight effects of the acceptance cuts. For a coupling to the Higgs proportional to the transverse tensor the same distribution peaks around $\Delta\phi_{jj} = 0, \pi$. This correlation can be used to determine the Lorentz structure of the $WWH$ coupling [52].

The modification to the $ggH$ coupling from a fourth generation leads to a larger relative size of the gluon-fusion process in the $H + 2$ jets sample. This causes a modification in the angular correlation, shown in Fig. 5. For our MADEVENT [53] simulation we employ all of the cuts listed in Ref. [54], except that we reduced the cut on the invariant mass of the jets to $m_{jj} > 200$ GeV (appropriate to Tevatron energies), and use the HEFT model [39]. Measuring this distribution would provide an interesting probe of the relative sizes of the weak vector boson fusion over gluon fusion. Of course this relative weight will be affected by cuts as well as analysis strategies like a minijet veto and requires a careful study.

New decay modes of the Higgs are possible if the Higgs is sufficiently heavy. Simply trying to produce the Higgs and decay to two heavy quarks at hadron colliders is small compared with the QCD production and therefore not promising. For decays to heavy leptons there are two cases to distinguish, depending on the size of the mixing between the fourth-generation leptons and the SM leptons.

One very interesting modification to Higgs signals occurs if the mixing between the fourth-generation leptons and the other generations is very small ($|U_{i4}| < 10^{-8}$). In this case, the fourth-generation neutrinos escape the detector as missing energy. This will be the case, for example, when one contemplates the fourth-generation neutrino as

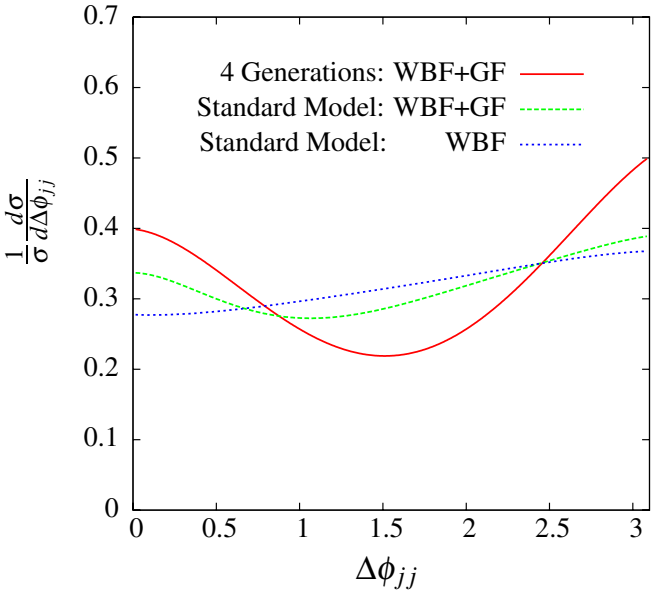


FIG. 5 (color online). Angular distribution of vector-boson fusion channel assuming reference point (b) with its Higgs mass $m_H = 200$ GeV.

dark matter. (The intermediate case of decay with a displaced vertex is also possible for a narrower range of PMNS mixings of roughly $10^{-6} \lesssim |U_{i4}| \lesssim 10^{-8}$. A recent discussion of the possibility of displaced vertices associated with Higgs decay to neutrinos, in a different context, can be found in [55].) LEP II bounds on missing energy plus an initial-state photon are relatively weak, and thus the fourth-generation neutrino can be as light as about $M_Z/2$. This case also requires a mechanism to avoid the direct detection bounds (we comment on this below) which otherwise rule out weak-scale Dirac neutrinos as dark matter. For Higgs masses below 140 GeV, the invisible decay $H \to \nu_4\bar{\nu}_4$ can even dominate. Such a signature is among the more challenging at the LHC, in particular, because the most likely channel to observe an invisible Higgs is weak-boson fusion, which is not enhanced by fourth-generation loop effects [51].

If the mixing $|U_{i4}|$ is not exceedingly small, then the fourth-generation neutrino promptly decays via a PMNS mixed charged current $U_{i4}\ell_i^{\pm}\nu_4 W^{\mp}$. Given the LEP bounds for this two-body decay to be open, the Higgs must be heavier than about 200 GeV. This means that the new signal is $H \to \nu_4\bar{\nu}_4 \to \ell^+\ell^- W^+ W^-$ where the lepton flavor depends on which PMNS mixing element dominates. The branching ratio of this mode, shown in Fig. 3, is roughly 5% for Higgs masses larger than the kinematic threshold. When combined with the branching ratio of the $W$'s into leptons, we can estimate that the rate into four leptons (plus missing energy)

$$\frac{\mathrm{BR}(H \to \nu_4\bar{\nu}_4 \to 4\ell)}{\mathrm{BR}(H \to ZZ \to 4\ell)} \simeq 1.1\left(\frac{\mathrm{BR}(H \to \nu_4\bar{\nu}_4)}{0.1}\right). \quad (14)$$

Hence, the rate is comparable to the rate for $H \to ZZ \to 4\ell$. One subtlety is that the decay $\nu_4 \to \ell W$ likely proceeds to third generation leptons, if indeed the PMNS mixing element $|U_{\tau 4}|$ is largest, and so the two leptons from this decay would be $\tau$'s. It might nevertheless be worthwhile to study the four lepton signal characteristics, including the relative rates into different lepton flavors, as well as searching for events with accompanying missing energy.

In the case where the fourth-generation neutrino has an electroweak scale Majorana mass, $M_{44} \sim v y^{\nu}_{44}$, half of the time the same two-body decay proceeds to same-sign leptons $H \to \nu_4\nu_4 \to \ell^{\pm}\ell^{\pm} W^{\mp} W^{\mp}$. This rather unusual signal of the Higgs, discussed in a similar context in Ref. [56], has little physics background except potentially Higgs pair production, with each Higgs decaying into $W$ pairs. The difference is that the four generation signal has no missing energy, and moreover, the visible mass of the events would approximately reconstruct the Higgs mass and not threshold-suppressed two-Higgs production.

Finally, Higgs pair production is resurrected by fourth-generation loop effects. While the SM production rate at the LHC might barely be sufficient to confirm the existence of a triple Higgs coupling $\lambda_{HHH}$ as predicted by the Higgs

potential [57], the enhancement of the effective $ggH$ and $ggHH$ couplings should allow for a proper measurement of $\lambda_{HHH}$. Enhancements to Higgs pair production using an operator approach was also recently considered in Ref. [58].

Total rates are notoriously difficult observables at hadron colliders, but the Higgs self-coupling can be beautifully extracted from the threshold behavior of the $gg \to HH$ amplitude. At threshold, this process is dominated by the two form factors $F_{\Delta,\Box}$ proportional to the metric tensor, which arise from the triangular and box diagrams (following the notation of Ref. [59]). In the low-energy limit [39] the box diagram's form factor proportional to the transverse tensor is suppressed by powers of the loop mass. The Higgs-coupling analysis makes use of the fact that at threshold the two contributions $F_\Delta$ and $F_\Box$ cancel. More precisely, in the low-energy limit $m_H \ll \sqrt{s} \ll m_t$ we find $F_\Delta = -F_\Box + \mathcal{O}(\hat{s}/m_t^2)$. This cancellation explains the increase in rate when we set $\lambda_{HHH}$ to zero, as shown in Table III.

If we only slightly vary the size of the Higgs self-coupling, this threshold behavior changes significantly [57] and provides an experimental handle on $\lambda_{HHH}$. In Fig. 6 we show the $HH$ invariant mass (or $\hat{s}$ at parton level) distribution. The shift between finite and zero $\lambda_{HHH}$ in the standard model provides the (S)LHC measurement of the Higgs self-coupling. Similarly to the $ggH$ form factors shown in Table II the decoupling assumption for top quarks is numerically not quite as good as for the additional fourth-generation quarks. Once the process is dominated by heavier quarks the variation of $m_{HH}$ with $\lambda_{HHH}$ becomes significantly more pronounced, so there is little doubt that we can use it to measure the Higgs self-coupling.

For the standard model, the Higgs self-coupling analysis at the LHC is likely restricted to the $4W$ decay channel [57]. From Table III we see that for light Higgs masses this decay is strongly suppressed, so it would be an interesting exercise to see if there are alternative decay channels [60] which might work for lighter Higgs bosons, given the rate and $m_{HH}$ sensitivity increase by the fourth generation.

TABLE III. Total cross section for Higgs pair production at the LHC for two different Higgs masses, 115 and 200 GeV according to reference points (a) and (b). All masses are given in units of GeV, all rates in units of fb.

| | $\lambda_{HHH}$ | $m_H$ | $\sigma_{gg\to HH}$ | $\sigma_{gg\to HH}\,\mathrm{BR}(4W)$ |
|---|---|---|---|---|
| SM | $\lambda_{\mathrm{SM}}$ | 115 | 34.07 | 0.22 |
| SM | 0 | 115 | 63.56 | 0.41 |
| SM | $\lambda_{\mathrm{SM}}$ | 200 | 8.54 | 4.61 |
| SM | 0 | 200 | 25.73 | 13.89 |
| (a) | $\lambda_{\mathrm{SM}}$ | 115 | 299.7 | 0.76 |
| (a) | 0 | 115 | 500.2 | 1.26 |
| (b) | $\lambda_{\mathrm{SM}}$ | 200 | 96.2 | 51.30 |
| (b) | 0 | 200 | 241.3 | 128.6 |

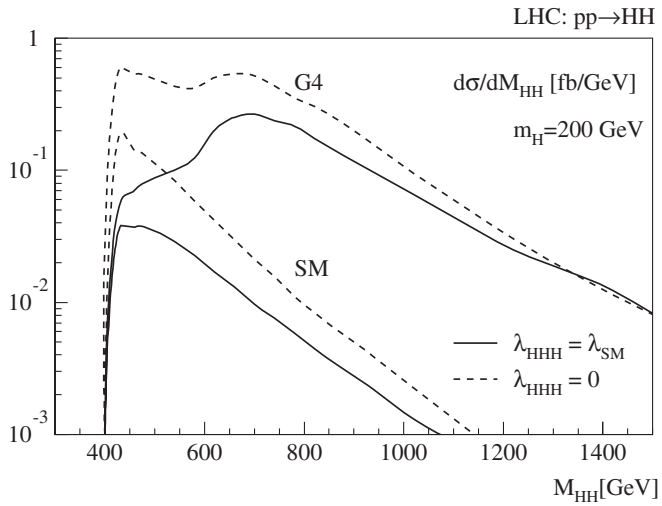


FIG. 6. Invariant mass distribution for Higgs pair production at the LHC. We show the standard model and fourth-generation curves in the reference point (b). For the dashed line the Higgs self-coupling is set to zero.

## V. METASTABILITY AND TRIVIALITY

Until now we have concentrated on collider effects of a fourth generation coupled to one Higgs doublet. Since the Yukawa couplings of the new fermions exceed 1.5 for the fourth-generation quarks, the four-generation model as an effective theory breaks down at a scale that may not be far above the TeV scale. There are two well-known constraints: (1) the possibility that the quartic coupling is driven negative, destabilizing the electroweak scale by producing large field minima through quantum corrections [61], and (2) large Yukawa couplings driving the Higgs quartic and/or the Yukawas themselves to a Landau pole, i.e., entering a strong-coupling regime.

In both cases the problematic coupling is the Higgs quartic, since it receives much larger new contributions to its renormalization group running from the fourth-generation quark Yukawas couplings. The renormalization group equation for $\lambda(\mu)$ is

$$16\pi^2 \frac{d\lambda}{dt} = 12\lambda^2 - 9\lambda g_2^2 - 3\lambda g_1^2 + 4\lambda \sum N_f y_f^2 - 4 \sum N_f y_f^4, \tag{15}$$

where we have shown only the dominant terms. The last two terms encode the Higgs wave function and quartic terms induced by the fermions; the sum is over all identical fermions with degeneracy $N_f$. In our numerical estimations we also include the subleading electroweak coupling dependence, and evolve using the full set of one loop $\beta$ functions [62].

We can estimate the scale at which the metastability bound becomes problematic by requiring that the probability of tunneling into another vacuum over the current age of the Universe is much less than 1. This is equivalent to the requirement that the running quartic interaction is [63]

$$\lambda(\mu) \lesssim \frac{4\pi^2}{3\ln(H/\mu)}, \tag{16}$$

where $H$ is the Hubble scale. The scale at which this inequality is saturated is a minimum scale where new physics is required. We should emphasize that the new physics does *not* need to be strongly coupled. For example, a supersymmetric model with four generations does not have a running quartic that turns negative as long as superpartners are (roughly) below the TeV scale. This is important because weakly coupled physics with particles obtaining their mass through, e.g., supersymmetry breaking, not electroweak breaking, will hardly affect our Higgs results.

The second constraint is potentially a stronger one. Requiring that the quartic remain perturbative, $\lambda(\mu) \lesssim 4\pi$, we find that the upper bound on the cutoff scale of the theory rapidly becomes small as the Higgs mass is increased. We show this constraint as well as the metastability constraint in Fig. 7. We find that for our choices of fourth-generation masses, the Yukawa interactions remain perturbative to slightly beyond the Higgs metastability/triviality bounds for all considered Higgs masses. The "chimney" region, in which the effective theory of the standard model with $m_{H_{\rm SM}} \sim 200$ GeV remains valid to $M_{\rm Pl}$, closes off. We find the maximal cutoff scale before new physics of any kind enters occurs for Higgs masses in the neighborhood of 300 GeV. Much lower Higgs masses, in particular $m_H < 2M_W$, imply other new physics must enter to prevent developing a deeper minimum away from the electroweak breaking vacuum. Nevertheless, we emphasize that this new physics can be weakly coupled below a TeV with little effect on Higgs physics itself.

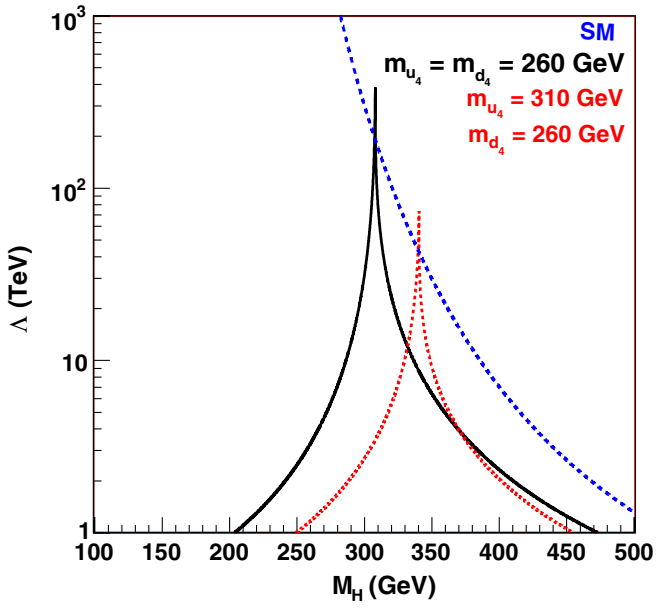


FIG. 7 (color online). The maximum scale at which new physics enters into the Higgs potential to avoid either a too short-lived vacuum or to avoid a Landau pole in $\lambda$. These two constraints are qualitatively distinct: metastability can be restored by *weakly* coupled physics below a TeV scale, whereas the Landau pole signals a strongly interacting Higgs sector. The dashed curve reproduces the SM triviality bound.

Conversely, to resolve the physics of the cutoff scale in the case where the quartic (or the Yukawas) encounter a Landau pole undoubtedly requires physics directly connected to electroweak symmetry breaking. This new physics could be stronger-coupled supersymmetry, technicolor, topcolor, or a little Higgs construction.

## VI. DISCUSSION

We have considered the constraints on a fourth generation and its effects on Higgs physics in the standard model. If nature does indeed have a fourth generation, it is amusing to speculate on the rich series of new phenomena expected at colliders now operating and about to begin. The ordering of discoveries could proceed by Tevatron discovering the Higgs, with an unusually large production cross section, or in mass range that was previously thought to be undetectable in the standard model. Subdominant decays of the Higgs may reveal a new sector. Direct production of fourth-generation neutrinos or leptons may also be possible at Tevatron, but relies on a more detailed understanding of the background. Once the LHC turns on, the fourth-generation quarks should be readily produced and found. The Higgs can be found using the golden mode for a wide range of mass, and for most of this range, it will be found very quickly with a small integrated luminosity (due to the large enhancement of the gluon fusion channel). Given measures of the cross section for Higgs production as well as branching ratios of Higgs into subdominant modes, the LHC will be able to rapidly verify that a fourth *chiral* generation does indeed exist.

While our focus has been on the *effects* of a fourth generation, there is also the possibility that a fourth generation could alleviate or solve some of the pressing problems addressed by other models of new physics. One amusing possibility is to employ a variation of the mechanism of Ref. [64] to revive electroweak baryogenesis in the (four-generation) standard model. Another possibility is to impose a parity symmetry to stabilize the fourth-generation lepton to serve as cold dark matter. This is naively ruled out by direct detection, however there are mechanisms [65,66] to avoid these bounds by either splitting the neutrino eigenstates with a small Majorana mass or otherwise invoking additional physics such as a $Z'$ coupling to

$U(1)_{B-L}$. A detailed study of these issues is in progress and will be reported on elsewhere.

## ACKNOWLEDGMENTS

We thank A. de Gouvêa, D. E. Kaplan, E. Katz, M. Schmaltz, and J. Wacker for discussions and C. Wagner for reminding us of the true and electroweak baryogenesis. G. D. K., T. P., and T. T. thank the Aspen Center of Physics for a stimulating atmosphere where this work was begun. G. D. K. thanks SUPA and Argonne National Laboratory for hospitality where part of this work was completed. This work was supported in part by the Department of Energy under Contracts No. DE-FG02-96ER40969 (G. D. K.) and No. DE-AC02-06CH11357 (T. T.).

[1] One could also speculate about five or more generations. Optimizing over particle masses, we find that the contribution to the oblique electroweak parameters is $\Delta S \simeq \Delta T \gtrsim 0.3$ and thus outside the 95% C.L. ellipse.
[2] W. M. Yao *et al.* (Particle Data Group), J. Phys. G **33**, 1 (2006).
[3] P. H. Frampton, P. Q. Hung, and M. Sher, Phys. Rep. **330**, 263 (2000).
[4] H. J. He, N. Polonsky, and S. f. Su, Phys. Rev. D **64**, 053004 (2001).
[5] M. Maltoni, V. A. Novikov, L. B. Okun, A. N. Rozanov, and M. I. Vysotsky, Phys. Lett. B **476**, 107 (2000).
[6] Direct search experiments have ruled out a stable fourth-generation Dirac neutrino with a cosmological relic density (as well as densities much lower than even this) [67]. Whether the thermal relic abundance can be arranged to sufficiently small so as to contribute insignificantly to cosmological dark matter (and thus avoid the direct search bounds) depends on how large the annihilation cross section can be made, which in turn depends on several parameters including the Majorana mass of the neutrino. See [66] for a recent discussion.
[7] V. A. Novikov, L. B. Okun, A. N. Rozanov, and M. I. Vysotsky, Phys. Lett. B **529**, 111 (2002).
[8] V. A. Novikov, L. B. Okun, A. N. Rozanov, and M. I. Vysotsky, Pis'ma Zh. Eksp. Teor. Fiz. **76**, 158 (2002) [JETP Lett. **76**, 127 (2002)].
[9] E. Arik, M. Arik, S. A. Cetin, T. Conka, A. Mailov, and S. Sultansoy, Eur. Phys. J. C **26**, 9 (2002).
[10] E. Arik, O. Cakir, S. A. Cetin, and S. Sultansoy, Phys. Rev. D **66**, 033003 (2002).
[11] J. M. Frere, A. N. Rozanov, and M. I. Vysotsky, Phys. At. Nucl. **69**, 355 (2006).
[12] E. Arik, O. Cakir, S. A. Cetin, and S. Sultansoy, Acta Phys. Pol. B **37**, 2839 (2006).
[13] B. Holdom, J. High Energy Phys. 08 (2006) 076; 03 (2007) 063; arXiv:0705.1736.
[14] W. Skiba and D. Tucker-Smith, Phys. Rev. D **75**, 115010 (2007).
[15] C. T. Hill and E. A. Paschos, Phys. Lett. B **241**, 96 (1990).
[16] J. Abdallah *et al.* (DELPHI Collaboration), Eur. Phys. J. C **50**, 507 (2007).
[17] The Tevatron also has sensitivity to the charged and neutral leptons, although there are several subtleties involving triggering (particularly when $p_T$ is small) and backgrounds. We are not aware of robust bounds from run II data (independently of PMNS flavor mixing, for example). However, it may be possible to eliminate some lepton mass parameter space for some or all flavor mixings with a careful analysis.
[18] http://www-cdf.fnal.gov/physics/new/top/2005/ljets/tprime/gen6/public.html.
[19] S. M. Oliveira and R. Santos, Phys. Rev. D **68**, 093012 (2003).
[20] M. Sher, Phys. Rev. D **61**, 057303 (2000).
[21] A. Arhrib and W. S. Hou, Phys. Rev. D **64**, 073016 (2001).
[22] T. Aaltonen *et al.* (CDF Collaboration), arXiv:0706.3264.
[23] E. Golowich, J. Hewett, S. Pakvasa, and A. A. Petrov, arXiv:0705.3650.
[24] W. S. Hou, R. S. Willey, and A. Soni, Phys. Rev. Lett. **58**, 1608 (1987); **60**, 2337 (1988); W. S. Hou, A. Soni, and H. Steger, Phys. Lett. B **192**, 441 (1987).
[25] J. L. Hewett, Phys. Lett. B **193**, 327 (1987); G. Eilam, J. L. Hewett, and T. G. Rizzo, Phys. Lett. B **193**, 533 (1987); J. L. Hewett and T. G. Rizzo, Mod. Phys. Lett. A **3**, 975 (1988).
[26] V. M. Abazov *et al.* (D0 Collaboration), Phys. Rev. Lett. **98**, 181802 (2007).
[27] F. Canelli *et al.* (CDF Collaboration), Preliminary Conference Note 8588, http://www-cdf.fnal.gov/physics/new/top/2006/SingleTop/ME_1FB/index.html;
[28] J. Alwall *et al.*, Eur. Phys. J. C **49**, 791 (2007).
[29] T. P. Cheng and L. F. Li, *Gauge Theory of Elementary Particle Physics* (Clarendon, Oxford, UK, 1984), p. 536.
[30] A. de Gouvêa, arXiv:0706.1732.
[31] P. Bamert, C. P. Burgess, and R. N. Mohapatra, Nucl. Phys. **B438**, 3 (1995).
[32] M. E. Peskin and T. Takeuchi, Phys. Rev. D **46**, 381 (1992).
[33] B. A. Kniehl, Nucl. Phys. **B352**, 1 (1991).
[34] J. Alcaraz *et al.* (ALEPH Collaboration), arXiv:hep-ex/0612034.
[35] The latest LEP EWWG fit to $S, T$ can be found at http://lepewwg.web.cern.ch/LEPEWWG/plots/summer2006/s06_stu_contours.eps. The best fit to data is $(S, T) = (0.038, 0.077)$ where the SM, defined by $m_t = 175$ GeV and $m_H = 150$ GeV, is at the origin $(S, T) = (0, 0)$. Readjusting the definition of $(S, T) = (0, 0)$ to $m_t = 170.9$ GeV [68] and $m_H = 115$ GeV shifts the ellipse by an amount $(+0.017, +0.037)$.
[36] E. Gates and J. Terning, Phys. Rev. Lett. **67**, 1840 (1991).
[37] B. A. Kniehl and H. G. Kohrs, Phys. Rev. D **48**, 225 (1993).

[38] J. F. Gunion, D. W. McKay, and H. Pois, Phys. Lett. B **334**, 339 (1994); Phys. Rev. D **53**, 1616 (1996).
[39] J. R. Ellis, M. K. Gaillard, and D. V. Nanopoulos, Nucl. Phys. **B106**, 292 (1976); M. A. Shifman, A. I. Vainshtein, M. B. Voloshin, and V. I. Zakharov, Yad. Fiz. **30**, 1368 (1979) [Sov. J. Nucl. Phys. **30**, 711 (1979)]; B. A. Kniehl and M. Spira, Z. Phys. C **69**, 77 (1995); for an overview, see, e.g., A. Djouadi, arXiv:hep-ph/0503172.
[40] A. V. Manohar and M. B. Wise, Phys. Lett. B **636**, 107 (2006).
[41] S. C. Hsu *et al.* (CDF Collaboration), arXiv:0706.2200.
[42] D0 Collaboration, http://www-d0.fnal.gov/Run2Physics/WWW/results/prelim/HIGGS/H21/H21F0_supplement.eps.
[43] T. Plehn, D. L. Rainwater, and D. Zeppenfeld, Phys. Lett. B **454**, 297 (1999); A. Alves, O. Eboli, T. Plehn, and D. L. Rainwater, Phys. Rev. D **69**, 075005 (2004).
[44] A. Djouadi, J. Kalinowski, and M. Spira, Comput. Phys. Commun. **108**, 56 (1998).
[45] Our results differ from Ref. [10] who found a more modest reduction in the $H \rightarrow \gamma\gamma$ mode.
[46] D. Phalen, B. Thomas, and J. D. Wells, Phys. Rev. D **75**, 117702 (2007).
[47] CMS TDR, Report No CERN/LHCC/2006-001, 2006.
[48] D. L. Rainwater and D. Zeppenfeld, Phys. Rev. D **60**, 113004 (1999); **61**, 099901 (2000); N. Kauer, T. Plehn, D. L. Rainwater, and D. Zeppenfeld, Phys. Lett. B **503**, 113 (2001).
[49] M. Dittmar and H. K. Dreiner, Phys. Rev. D **55**, 167 (1997).
[50] V. Büscher and K. Jakobs, Int. J. Mod. Phys. A **20**, 2523 (2005).
[51] O. J. P. Eboli and D. Zeppenfeld, Phys. Lett. B **495**, 147 (2000).
[52] T. Plehn, D. L. Rainwater, and D. Zeppenfeld, Phys. Rev. Lett. **88**, 051801 (2002); V. Hankele, G. Klamke, D. Zeppenfeld, and T. Figy, Phys. Rev. D **74**, 095001 (2006).
[53] J. Alwall *et al.*, arXiv:0706.2334.
[54] V. Del Duca, W. Kilgore, C. Oleari, C. R. Schmidt, and D. Zeppenfeld, arXiv:hep-ph/0109147.
[55] M. L. Graesser, Phys. Rev. D **76**, 075006 (2007); arXiv:0705.2190.
[56] A. Datta and A. Pilaftsis, Phys. Lett. B **278**, 162 (1992); A. Datta, M. Guchait, and A. Pilaftsis, Phys. Rev. D **50**, 3195 (1994).
[57] U. Baur, T. Plehn, and D. L. Rainwater, Phys. Rev. Lett. **89**, 151801 (2002); Phys. Rev. D **67**, 033003 (2003); see also F. Gianotti *et al.*, Eur. Phys. J. C **39**, 293 (2005).
[58] A. Pierce, J. Thaler, and L. T. Wang, J. High Energy Phys. 05 (2007) 070.
[59] T. Plehn, M. Spira, and P. M. Zerwas, Nucl. Phys. **B479**, 46 (1996); **B531**, 655 (1998).
[60] U. Baur, T. Plehn, and D. L. Rainwater, Phys. Rev. D **69**, 053004 (2004).
[61] M. Sher, Phys. Rep. **179**, 273 (1989).
[62] H. Arason, D. J. Castano, B. Keszthelyi, S. Mikaelian, E. J. Piard, P. Ramond, and B. D. Wright, Phys. Rev. D **46**, 3945 (1992).
[63] G. Isidori, G. Ridolfi, and A. Strumia, Nucl. Phys. **B609**, 387 (2001).
[64] M. Carena, A. Megevand, M. Quiros, and C. E. M. Wagner, Nucl. Phys. **B716**, 319 (2005).
[65] D. R. Smith and N. Weiner, Phys. Rev. D **64**, 043502 (2001).
[66] G. Belanger, A. Pukhov, and G. Servant, arXiv:0706.0526.
[67] G. Servant and T. M. P. Tait, New J. Phys. **4**, 99 (2002).
[68] Tevatron Electroweak Working Group, arXiv:hep-ex/0703034.